Supporting Information for

Facet-engineered CeO_2 with Cu single atom drives photocatalytic selective oxidation of 5-hydroxymethylfurfural

Yifei Li, Senyao Meng, Ping Wang, Miao He, Jiasai Yao, Cheng Yang, Fangzhou Mo, Jiang Li * and Zhenxing Li*
State Key Laboratory of Heavy Oil Processing, China University of Petroleum, Beijing 102249, People's Republic of China

*corresponding author
E-mail address: lizx@cup.edu.cn (Z. Li); lijiang@cup.edu.cn (J. Li).

Experimental Section

Synthesis of ceria nanorod (CeO_2-R) and nanocube (CeO_2-C)

A total of 1.736 g of $Ce(NO)_3{\cdot}6H_2O$ and 19.2 g of NaOH were dissolved in 10 and 70 mL of deionized water, respectively[1]. After two solutions were mixed, it was continually stirred for 30 min. This mixed solution then was transferred into a Teflon-lined stainless-steel autoclave and hydrothermally treated at 373 and 453 K for 24 h to get CeO_2-R and CeO_2-C, respectively. The formed solids were separated by centrifugation and washed with deionized water and ethanol several times, followed by drying at 353 K for 8 h and calcining in air at 673 K for 4 h.

Synthesis of ceria octahedron (CeO_2-O)

A total of 0.858 g of $Ce(NO)_3{\cdot}6H_2O$ and 0.0076 g of Na_3PO_4 were dissolved in 10 and 70 mL of deionized water, respectively[2]. After two solutions were mixed and it was continually stirred for 30 min, this mixed solution was transferred into a Teflon-lined stainless steel autoclave and hydrothermally treated at 443 K for 10 h. After being cooled to room temperature, the formed solids were separated by centrifugation and washed with deionized water and methanol several times, then dried at 353 K for 8 h and calcined in air at 673 K for 4 h.

Facet-selective photo-deposition of metals or oxides

CeO_2 sample was synthesised by a hydrothermal procedure. For the facet-selective photo-depositions, two ways containing single reduction and single oxidation were carried out at room temperature without pH value adjusted. Normally, 0.50 g CeO_2 powder and a calculated amount of metal precursors (5 wt%) were mixed in 100 mL deionised water. The suspension was then irradiated by a 300-W Xe lamp (λ≥420 nm) under continuous stirring. After 5 h photo-deposition, the suspension was filtered, washed with deionised water for more than three times, and finally dried at 60 °C for overnight to obtain Pt/CeO_2 and PbO/CeO_2 samples. The as-obtained powder was used for characterization.

Photoelectrochemical performance

The photoelectrochemical test was performed in a 0.5 M Na_2SO_4 electrolyte solution using a three-electrode system. Disperse 5 mg the prepared catalyst and 20 μL 5 wt% Nafion solution in 500 μL water and 500 μL ethanol, and then sonicate for 1 h. Then 10 μL catalyst ink was dropped on the glassy carbon electrode and dried at room temperature. The obtained glassy carbon electrode, Ag/AgCl (saturated KCl) and platinum foil (1×1 cm^2) were used as working electrode, reference electrode and counter electrode, respectively, and were collected in the electrochemical station (CHI760E, China). A 300W Xe lamp was used as the visible-light source and was positioned 10 cm away from the electrode. Switching Xe lamps on and off every 50 seconds to obtain photochemical characteristics. The transient photocurrent responses were tested under chopped light irradiation (on/off cycle) at a polarization potential of 1.1 V (vs Ag/AgCl) and the sampling frequency of 10 Hz. The initial potential was set as an open circuit potential. Electrochemical impedance and Mott–Schottky measurements were performed in a three-electrode system under the same conditions. EIS measurements were carried out at the open circuit potential. The sample was coated onto a the FTO glass electrode, which was used as working electrode. Pt wire and Ag/AgCl (saturated KCl) were served as counter-electrode and reference electrode, respectively, 0.5 M Na_2SO_4 aqueous solution was used as the electrolyte.

The photocatalytic oxidation performance of HMF

In the catalytic reaction, 5-hydroxymethylfurfural (HMF) was selectively oxidized to 2, 5-dimethylfuran (DFF) by atmospheric O_2 under the irradiation of 300W Xenon lamp (Beijing ChangTuo Ltd., China). The distance between the light source and the center of the reaction solution is approximately 10 cm. The reaction solution temperature

was kept at around 30 °C by using cooling water. The initial HMF concentration and volume of suspension(benzotrifluoride was used as the reaction solvent) is 1 mM and 10 mL respectively. Before switching on the lamp, the suspension containing 80 mg catalyst was stirred for 30 min in the dark to attain the thermodynamic equilibrium. The suspension was diluted with methanol in a 1:5 ratio. The quantitative analysis of reactants and products was performed on a high performance liquid chromatography (HPLC) equipped with a C18 AQ column using a eluent consisted of 30 % methanol and 70 % ammonium formate (5 mM) at a flow rate of 0.5 mL/min. The column oven temperature was kept at 35 °C. The retention time of FFCA, HMF and DFF were 5.3, 9.5 and 10.9 min, respectively. The HMF conversion and DFF yield are calculated as follows:

$$\text{HMF conversion (\%)} = [n\text{ (HMF consumed)} / n\text{ (HMF initial)}] \times 100$$

$$\text{DFF yield (\%)} = [n\text{ (DFF formed)} / n\text{ (HMF initial)}] \times 100$$

The TOF value is calculated by the following expression: TOF= (number of moles of reactant converted (mol))/ (number of moles of catalyst (mol) ×time (h)). In Cu/CeO_2-R photocatalytic cycle test. Our photocatalytic test time takes 0.5 hours as a cycle, and the average yield within 0.5 hours is used as the evaluation standard. Centrifuge to obtain the reacted Cu/CeO_2-R. Then the photocatalyst was washed twice with deionized water. Dry in vacuum at 60 °C for 6 h, followed by placing it in a tubular furnace for calcination using a mixture of hydrogen and argon gases. Then continue to complete the photocatalytic reaction cycle test. The detection of H_2O_2 followed a previously reported iodometry method[3].

FTIR testing Detailed characterization procedure for HMF-adsorption in suit DRIFT

Before HMF adsorption, a pretreatment was conducted on a 2 mg sample. The catalyst was dissolved in ethanol along with a small amount of Nafion solution, and then dropped onto a silicon crystal. Nitrogen gas was introduced into the infrared device, and the infrared cell was cooled with liquid nitrogen to collect the background spectrum. The catalyst was placed in a trifluorotoluene solution and exposed to O_2 gas for HMF adsorption, and the infrared spectrum of the catalyst was collected. The reaction time was extended, and the infrared spectrum of the catalyst was collected.

DFT computations

DFT calculation details. The VASP software code to perform spin-polarized density functional theory (DFT) calculations. The ion-electron interactions are described using the projected enhanced wave (PAW) method, and the electron exchange effects and associated energies are approximately solved within the generalized gradient with the Perdew Burke-Ernzerhof form (GGA-PBE). All calculated plane-wave fundamental energy cutoffs were set to 400 eV. The atomic coordinates are completely relaxed until the maximum force on each atom is less than 0.05 eV/Å, and the energy convergence condition is 10^{-6} eV. The Cu/CeO_2 composite catalyst was simulated by Ce-O bond and Cu-O bond. The Brillouin zone was sampled at Gamma point with the 2×2×1 k-point meshes for all calculations. For all the models, we have set the vacuum space of 16 Å along the z-axis to guarantee sufficient space for geometry relaxation and intermediate adsorptions. All the atoms were allowed to be relaxed during the geometry optimization.

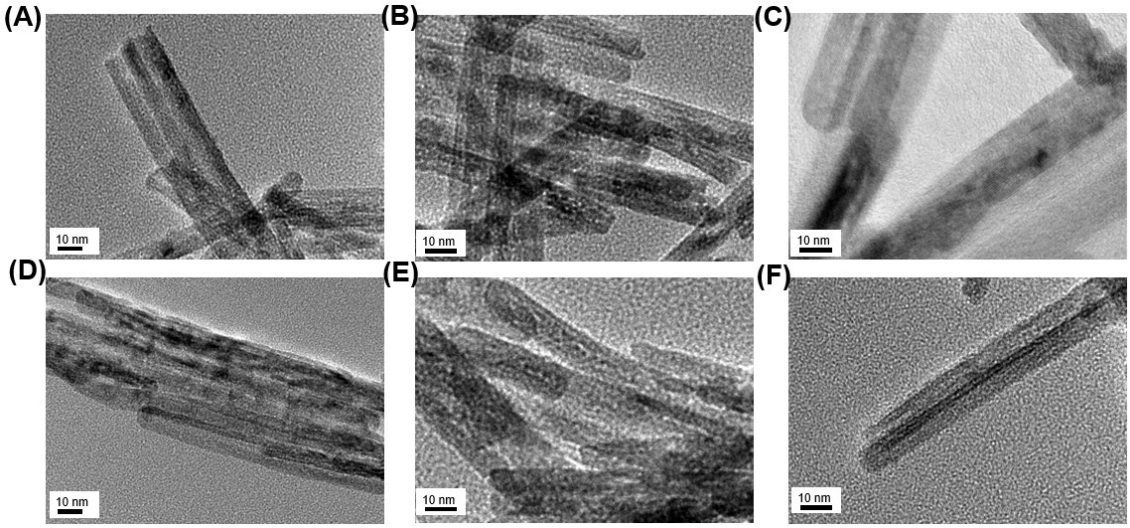

Fig. S1. HRTEM images of Cu/CeO_2-R.

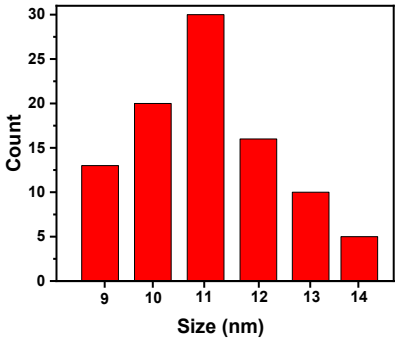

Fig. S2. Diameter distribution diagram of Cu/CeO_2-R.

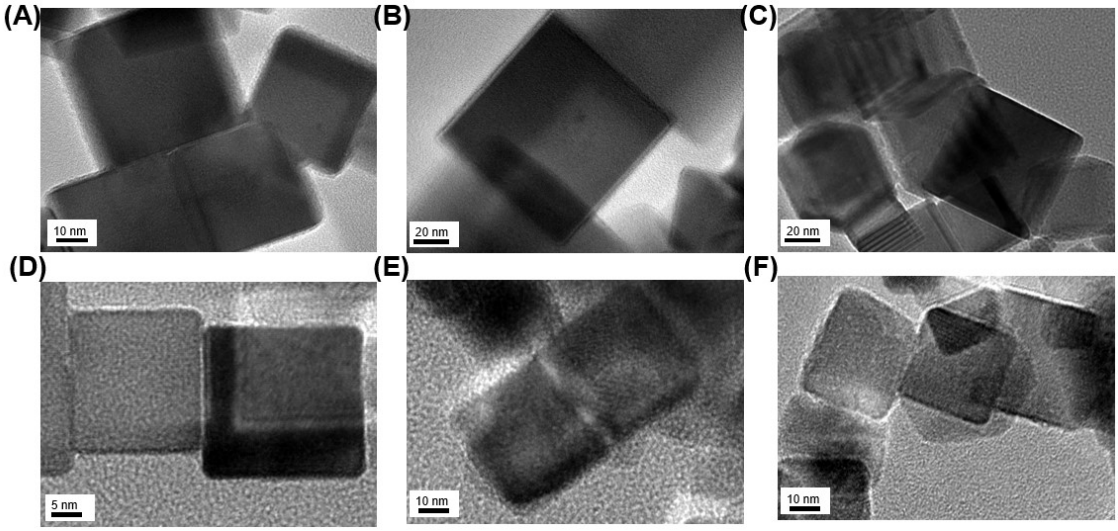

Fig. S3. HRTEM images of Cu/CeO_2-C.

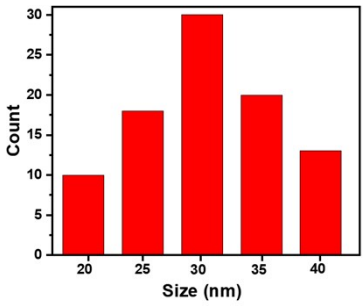

Fig. S4. Diameter distribution diagram of Cu/CeO_2-C.

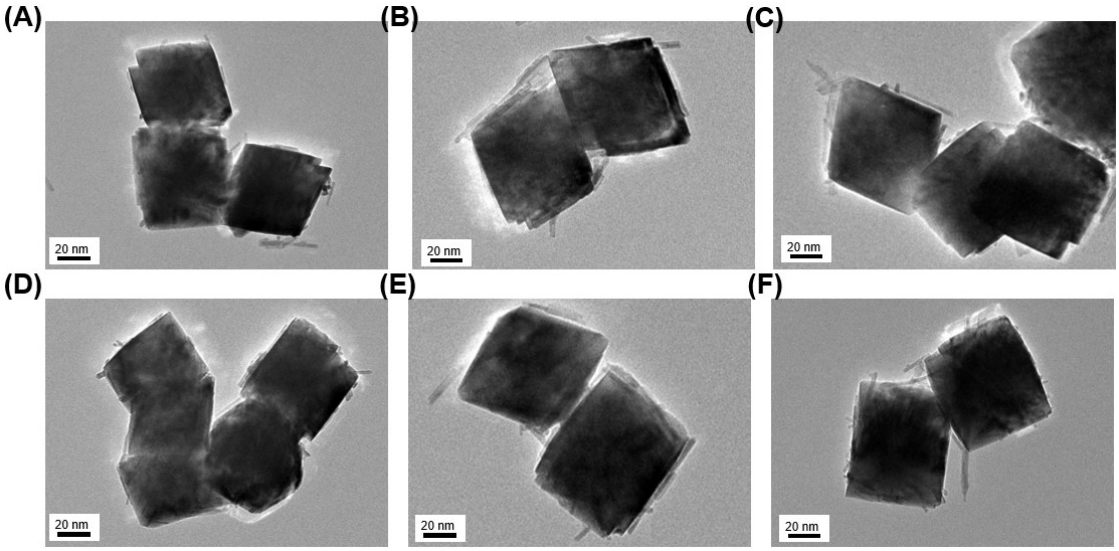

Fig. S5. HRTEM images of Cu/CeO_2-O.

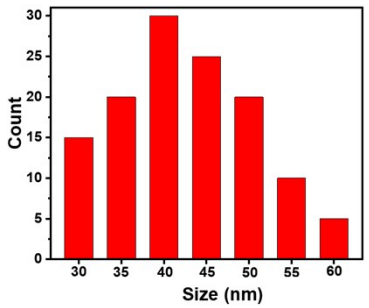

Fig. S6. Diameter distribution diagram of Cu/CeO_2-O.

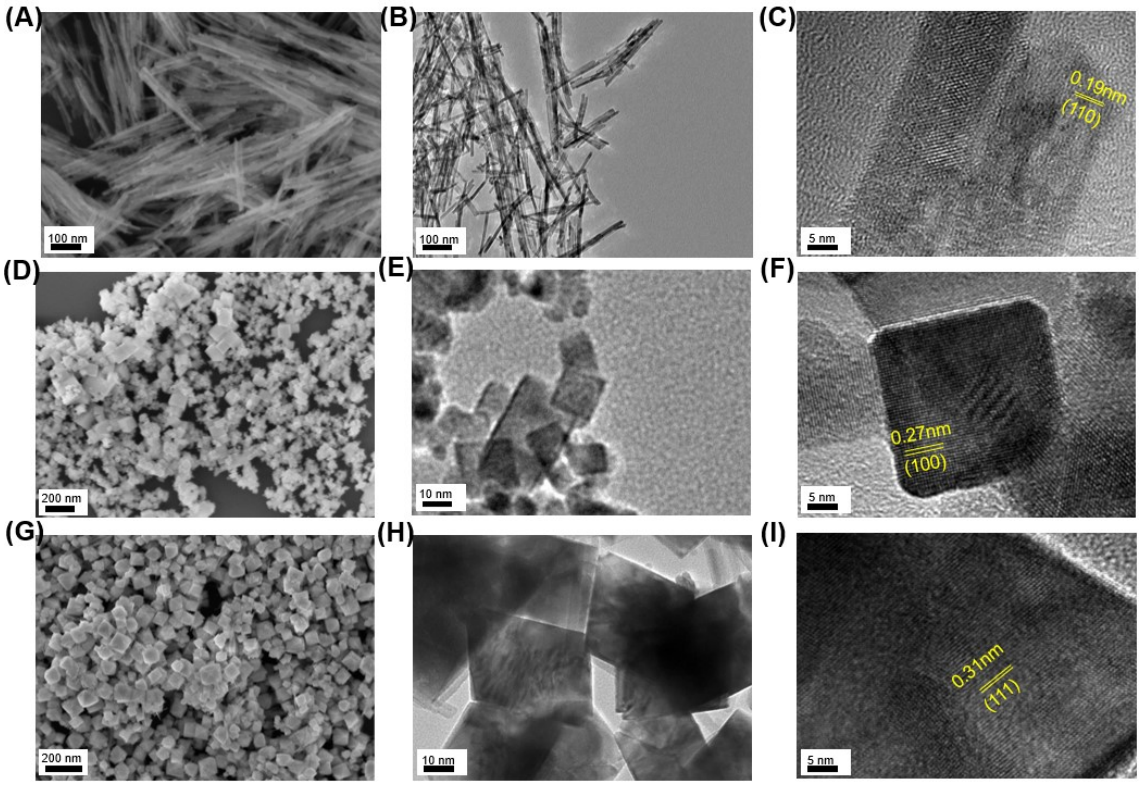

Fig. S7. SEM images of (A) CeO_2-R (D) CeO_2-C and (H) CeO_2-O. TEM images of (B) CeO_2-R (E) CeO_2-C and (H) CeO_2-O. HRTEM images of (C) CeO_2-R (F) CeO_2-C and (I) CeO_2-O.

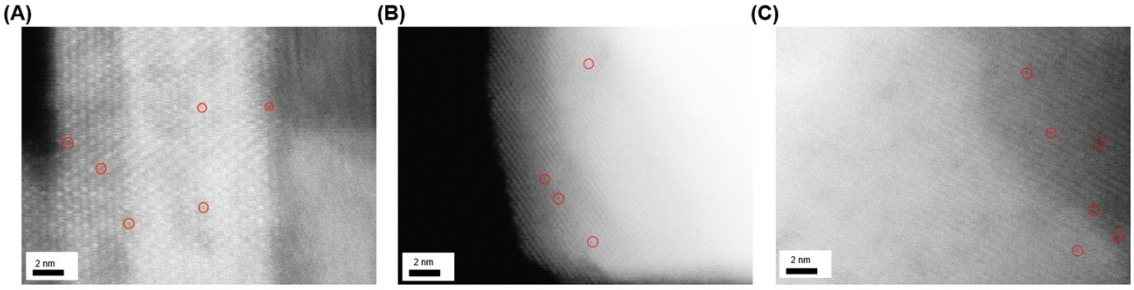

Fig. S8. AC-HAADF-STEM images of (A) Cu/CeO_2-R (B) Cu/CeO_2-C and (C) Cu/CeO_2-O

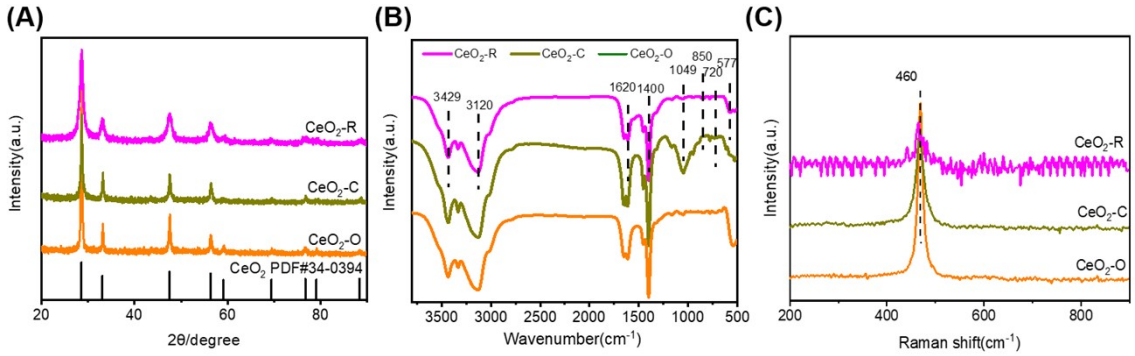

Fig. S9. (A) XRD patterns. (B) FTIR spectra. (C) Raman spectra.

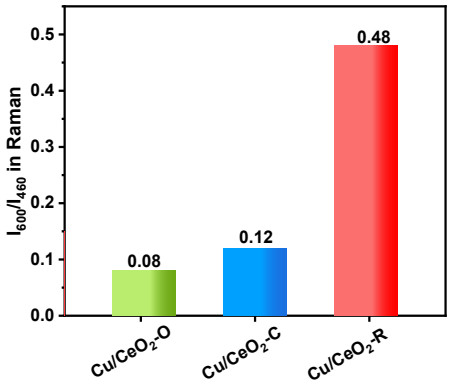

Fig. S10. Ratios of the intensities of the peaks at 600 and 460 cm^{-1} in Raman.

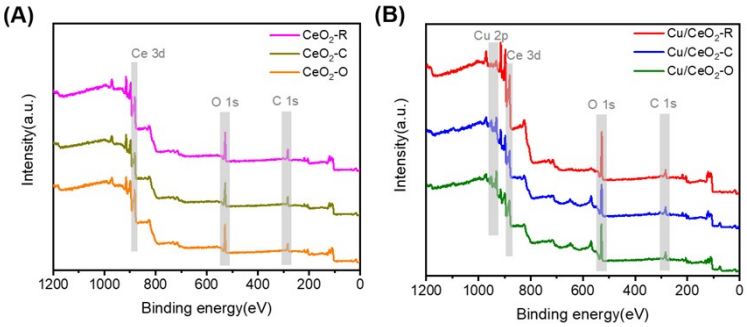

Fig. S11. Full spectra analysis of (A) CeO_2 and (B) Cu/CeO_2.

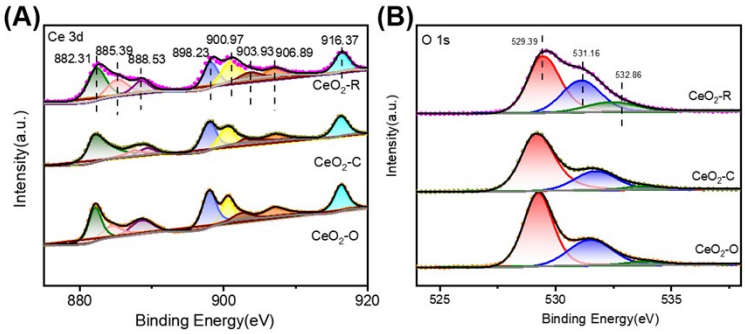

Fig. S12. XPS spectra of (A) Ce 3d, (B) O 1s of CeO_2-R, CeO_2-C and CeO_2-O.

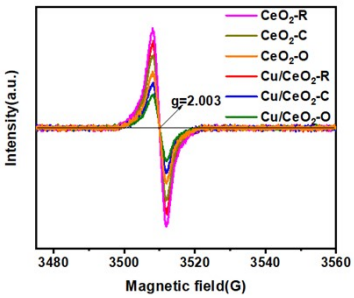

Fig. S13. EPR of catalysts.

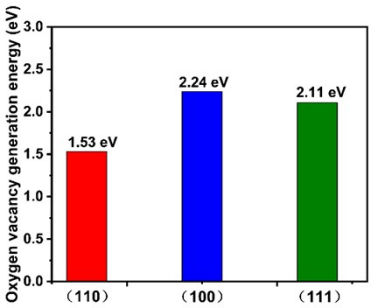

Fig. S14. Oxygen generation energy of crystal facet.

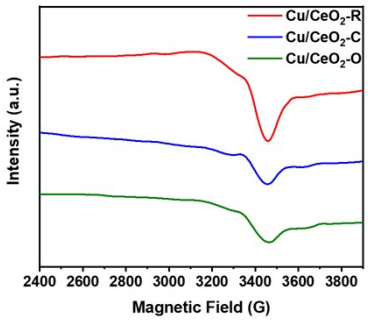

Fig. S15. EPR spectra of Cu/CeO_2 for Cu(Ⅱ).

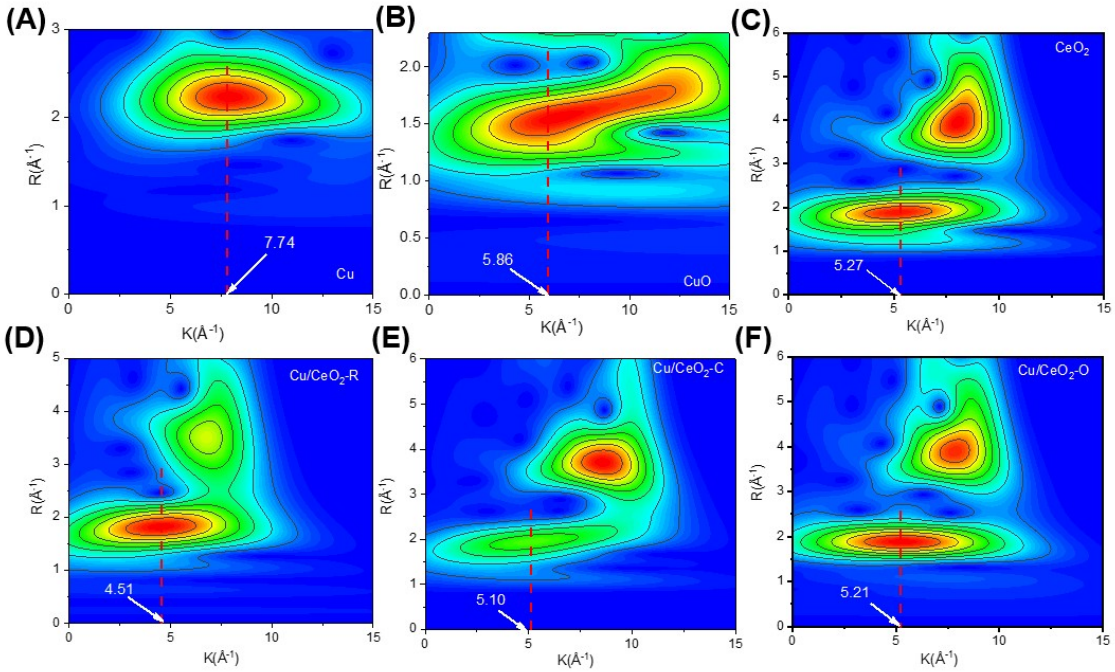

Fig. S16. Wavelet transforms analysis for (A)Cu, (B) CuO, (C) CeO_2, (D) Cu/CeO_2-R, (E) Cu/CeO_2-C and (F) Cu/CeO_2-O.

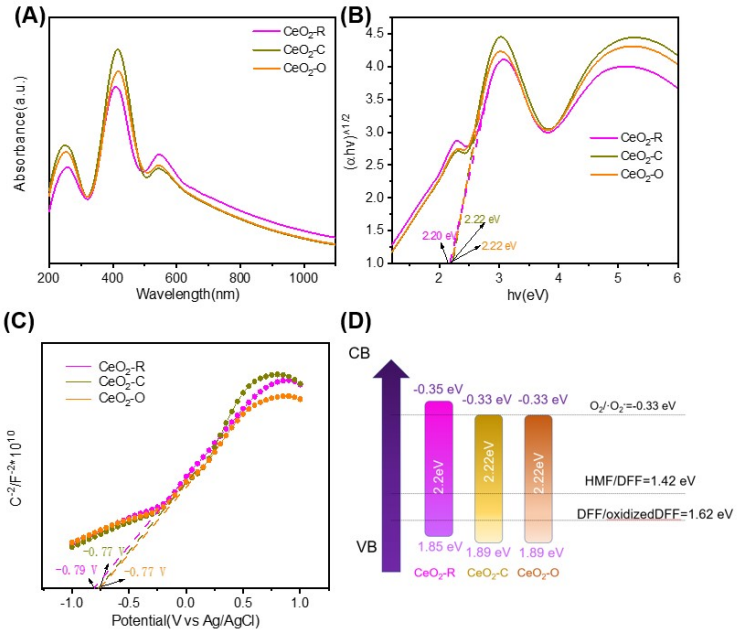

Fig. S17. (A) UV-vis spectra. (B) Tauc plots. (C) Corresponding Mott-Schottky plots. (D) Schematic diagram of the energy band structure of CeO_2-R, CeO_2-C and CeO_2-O.

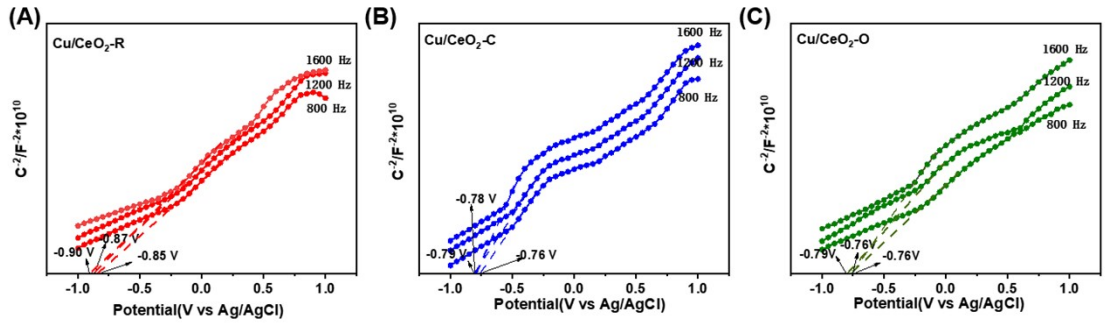

Fig. S18. Corresponding Mott-Schottky plots at (A) 800 Hz, (B) 1200 Hz, (C) 1600 Hz of Cu/CeO_2-R, Cu/CeO_2-C and Cu/CeO_2-O.

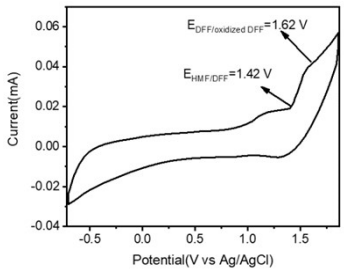

Fig. S19. The cyclic voltammetry graph of HMF.

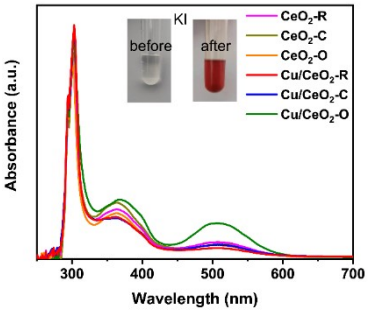

Fig. S20. UV-vis absorption spectra of excess saturated KI and appropriate amount of hydrochloric acid were added to the catalytic reaction solution.

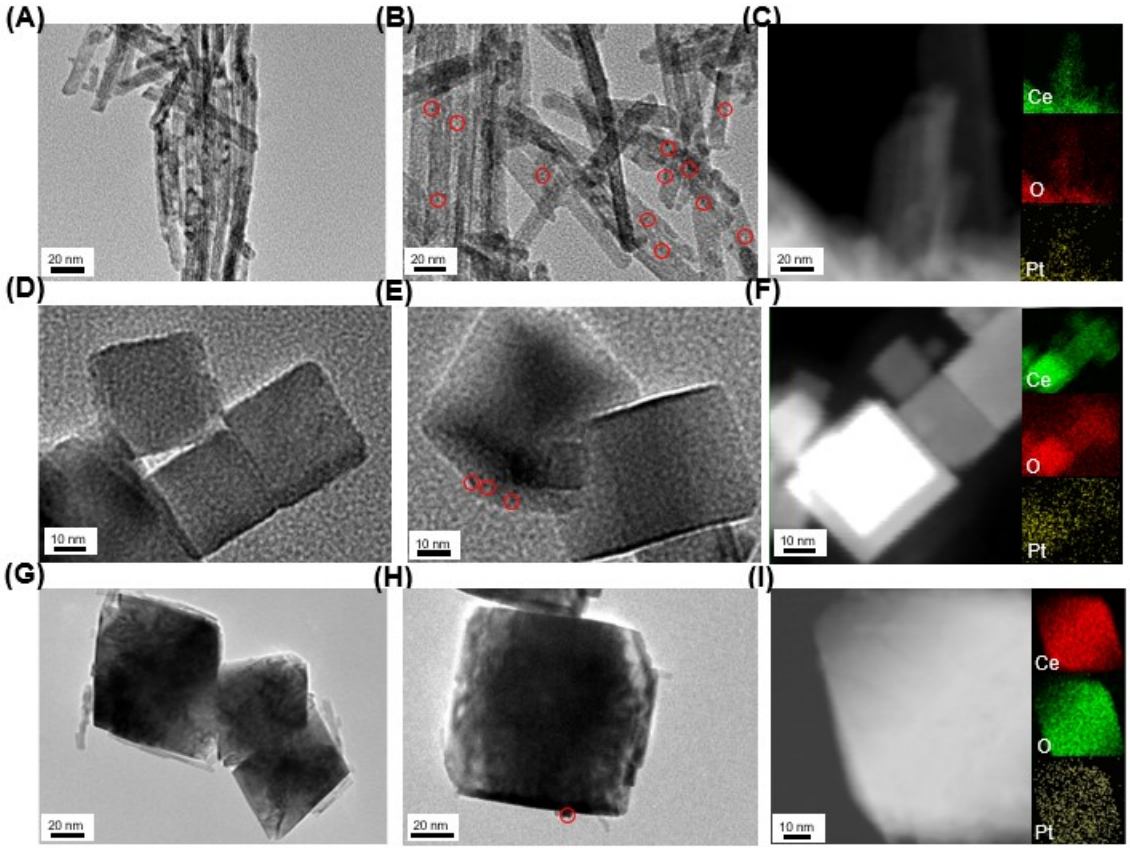

Fig. S21. TEM images of (A,B) Pt/CeO_2-R. (D,E) Pt/CeO_2-C. (G,H) Pt/CeO_2-O. EDS mappings of (C) Pt/CeO_2-R. (F) Pt/CeO_2-C. (I) Pt/CeO_2-O.

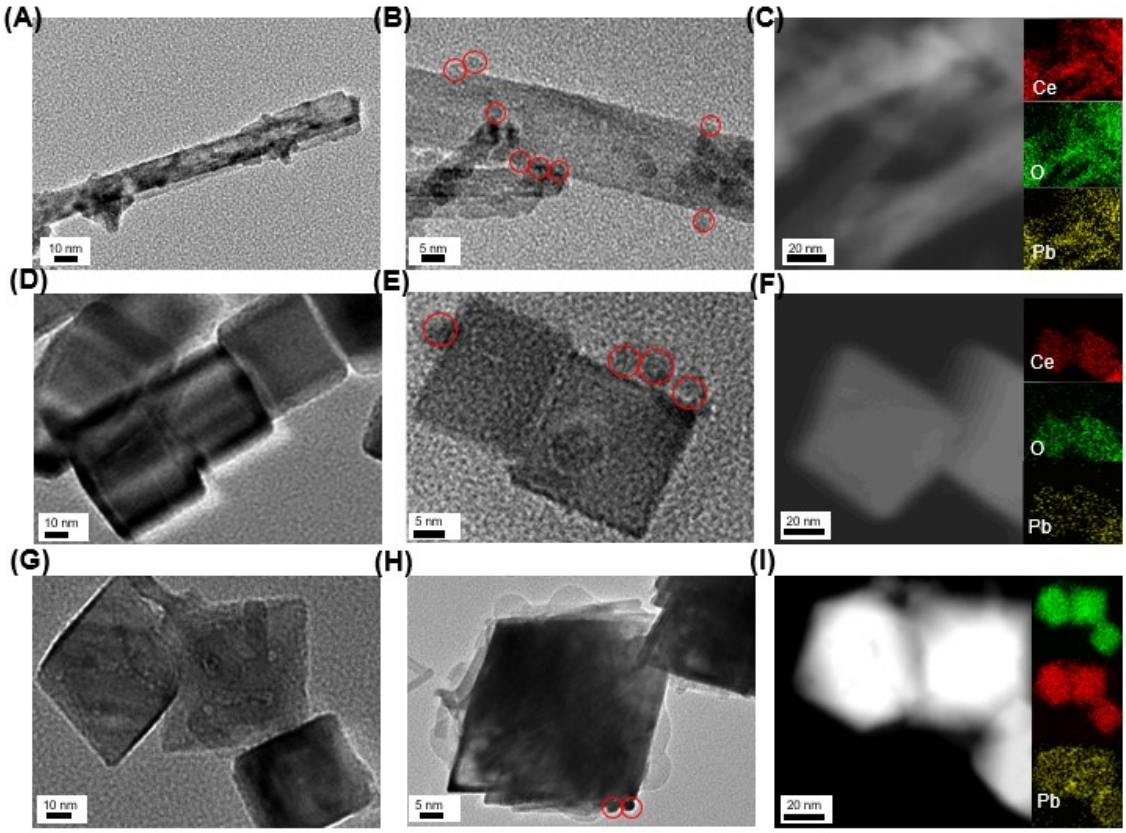

Fig. S22. TEM images of (A,B) PbO/CeO_2-R. (D,E) PbO/CeO_2-C. (G,H) PbO/CeO_2-O. EDS mappings of (C) PbO/CeO_2-R. (F) PbO/CeO_2-C. (I) PbO/CeO_2-O.

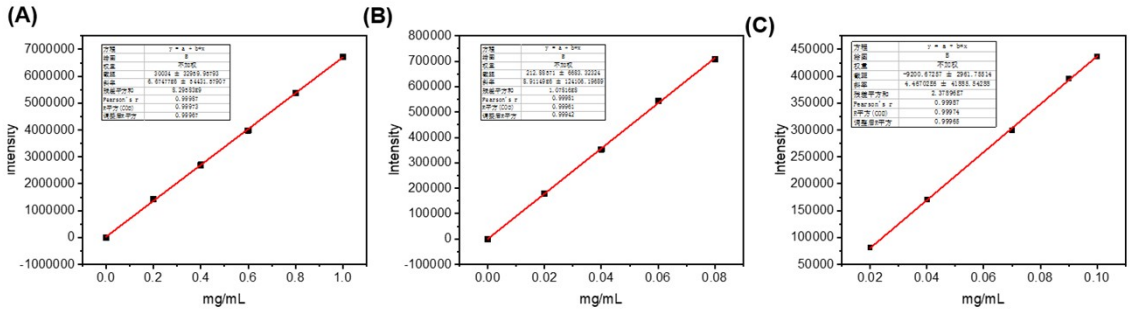

Fig. S23. Standard curve for (A)HMF(B)DFF(C)FFCA (diluted in methanol at a ratio of 1:5).

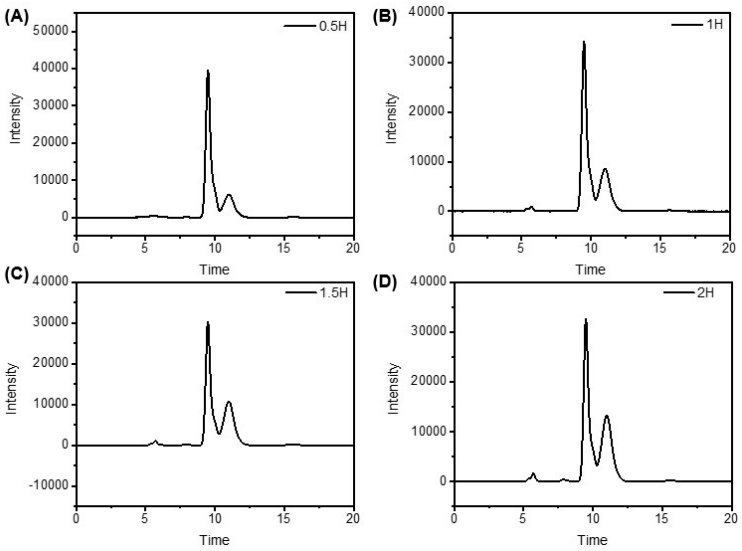

Fig. S24. The evolution for Cu/CeO_2-R.

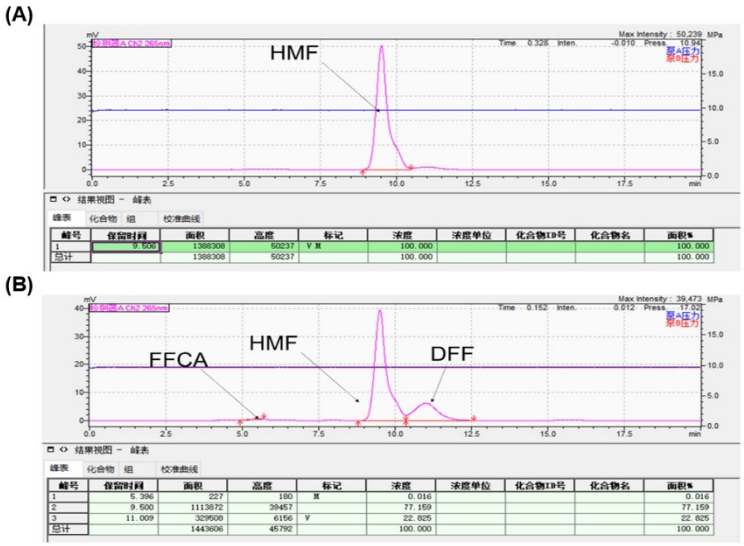

Fig. S25. Liquid-phase diagrams at (A)0 minute and (B)30 minutes for Cu/CeO_2-R.

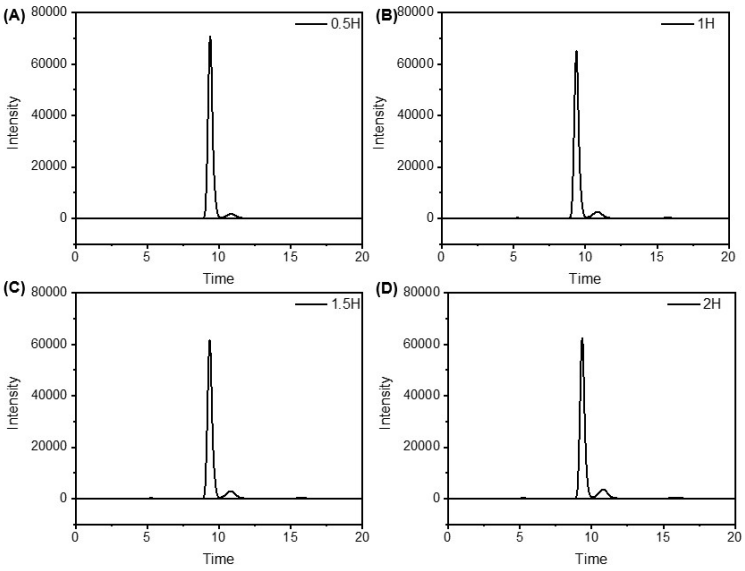

Fig. S26. The evolution process for Cu/CeO_2-C.

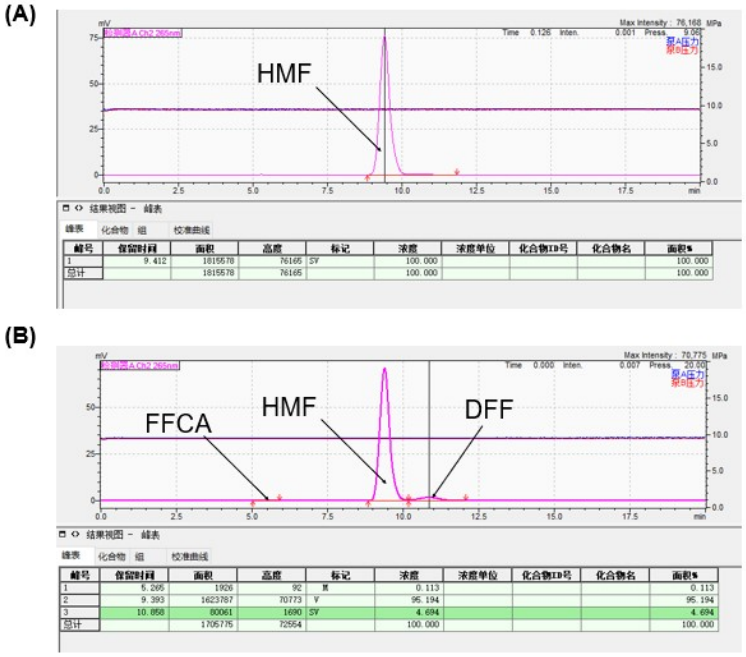

Fig. S27. Liquid-phase diagrams at (A)0 minute and (B)30 minutes for Cu/CeO_2-C.

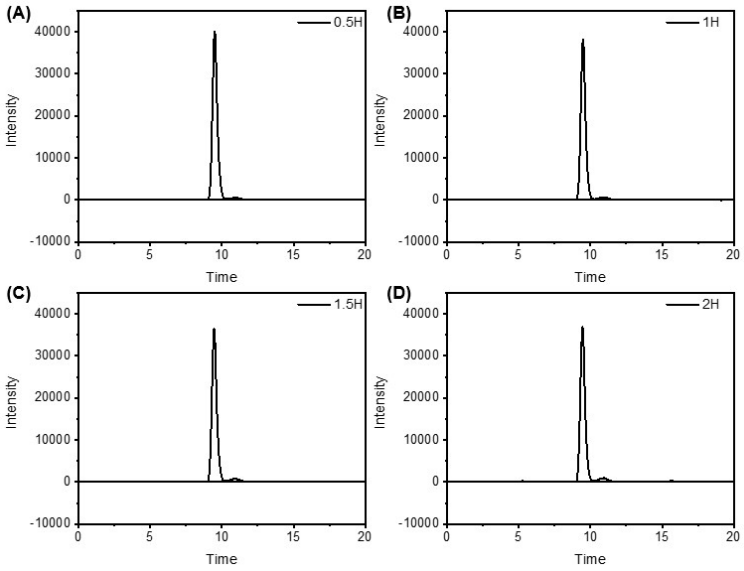

Fig. S28. The evolution process for Cu/CeO_2-O.

(a)

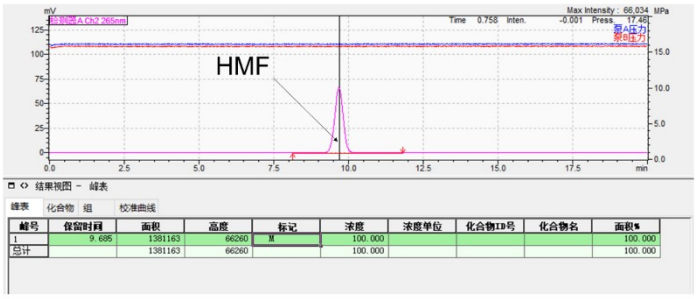

峰号	保留时间	面积	高度	标记	浓度	浓度单位	化合物ID号	化合物名	面积%
1	9.685	1381163	66260	M	100.000				100.000
总计		1381163	66260		100.000				100.000

(b)

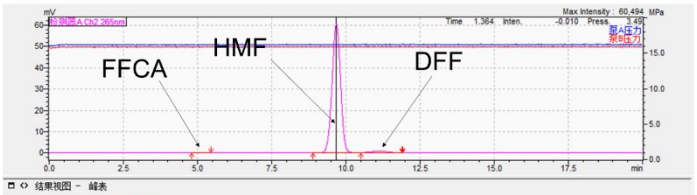

峰号	保留时间	面积	高度	标记	浓度	浓度单位	化合物ID号	化合物名	面积%
1	5.382	60	40	M	0.005				0.005
2	9.683	1229297	60493	S	97.622				97.622
3	11.166	29889	751	TV	2.374				2.374
总计		1259246	61284		100.000				100.000

Fig. S29. Liquid-phase diagrams at (A)0 minute and (B)30 minutes for Cu/CeO_2-O.

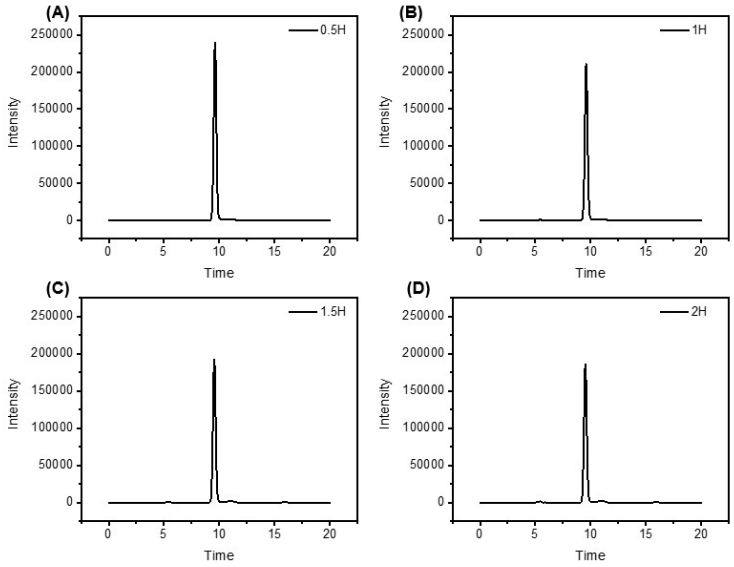

Fig. S30. The evolution process for CeO_2-R.

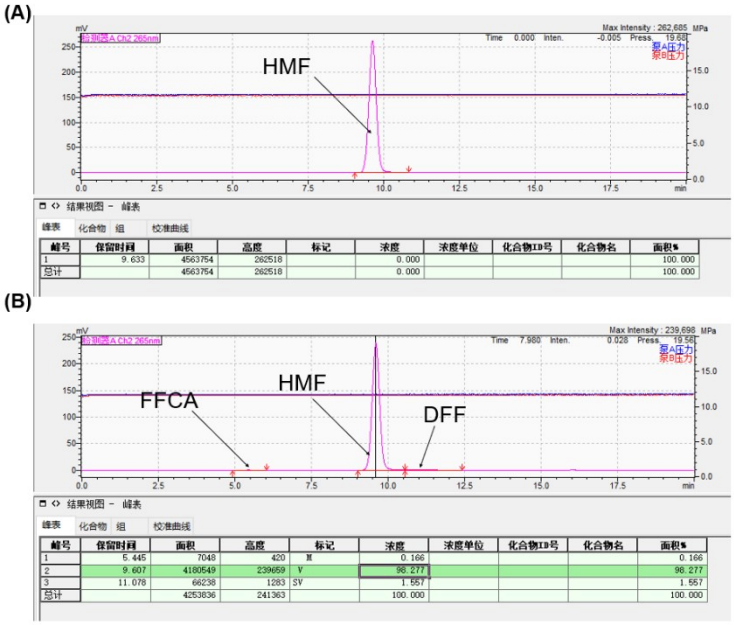

Fig. S31. Liquid-phase diagrams at (A)0 minute and (B)30 minutes for CeO_2-R.

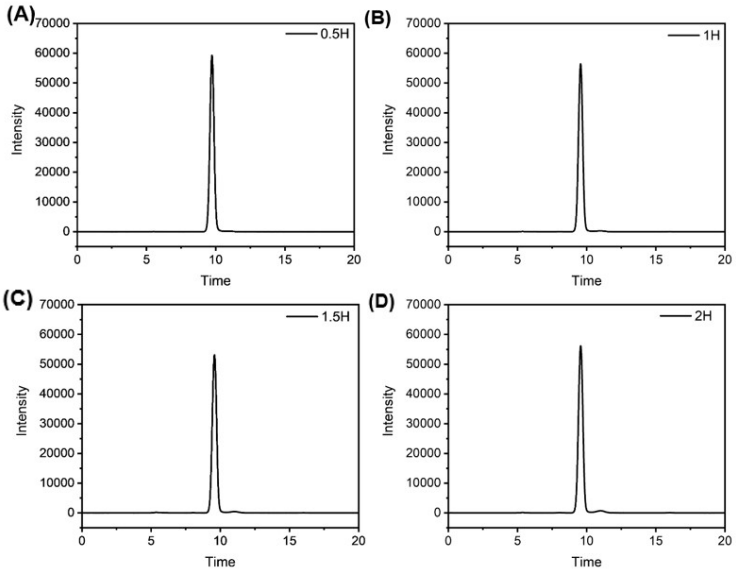

Fig. S32. The evolution process for CeO_2-C.

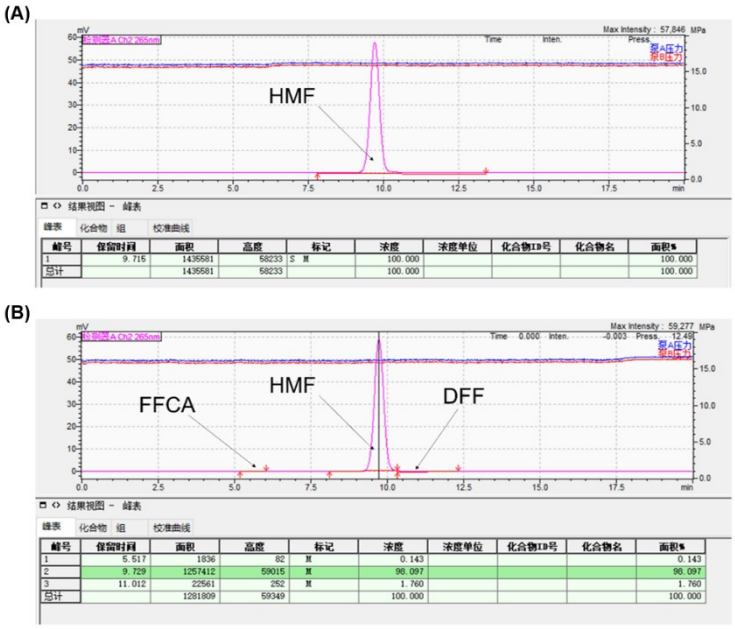

Fig. S33. Liquid-phase diagrams at (A)0 minute and (B)30 minutes for CeO_2-C.

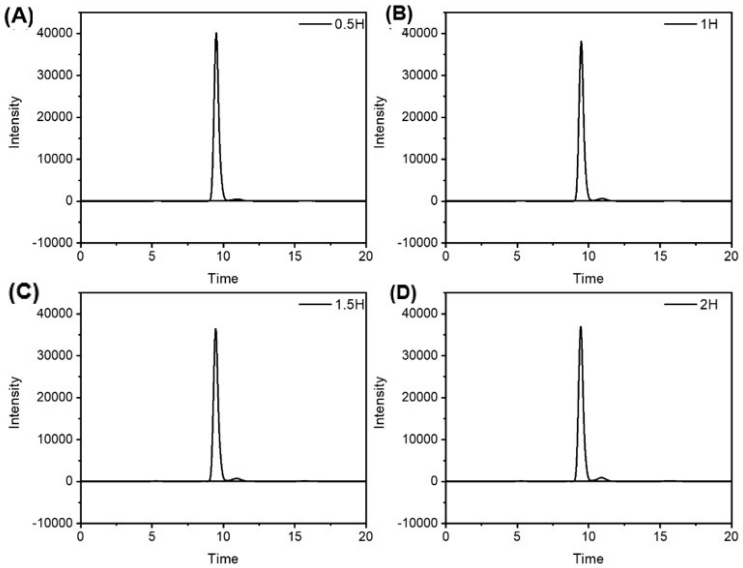

Fig. S34. The evolution process for CeO_2-O.

(A)

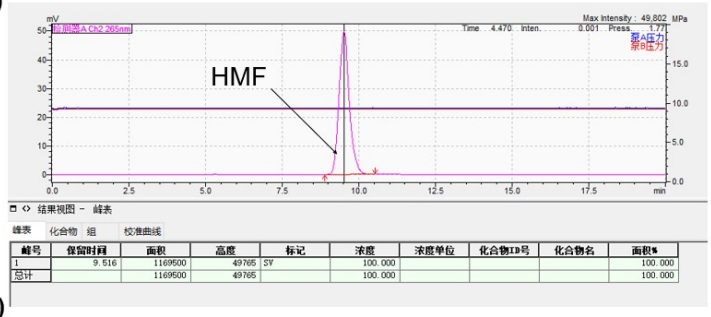

结果视图 - 峰表

峰表 化合物 组 校准曲线

峰号	保留时间	面积	高度	标记	浓度	浓度单位	化合物ID号	化合物名	面积%
1	9.516	1169500	49765	SV	100.000				100.000
总计		1169500	49765		100.000				100.000

(B)

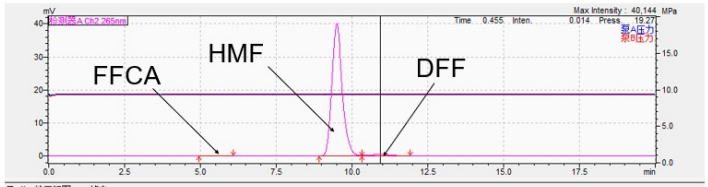

结果视图 - 峰表

峰表 化合物 组 校准曲线

峰号	保留时间	面积	高度	标记	浓度	浓度单位	化合物ID号	化合物名	面积%
1	5.273	1089	64	H	0.111				0.111
2	9.499	959424	40116		97.567				97.567
3	10.936	22839	465	SV	2.323				2.323
总计		983351	40644		100.000				100.000

Fig. S35. Liquid-phase diagrams at (A)0 minute and (B)30 minutes for CeO_2-O.

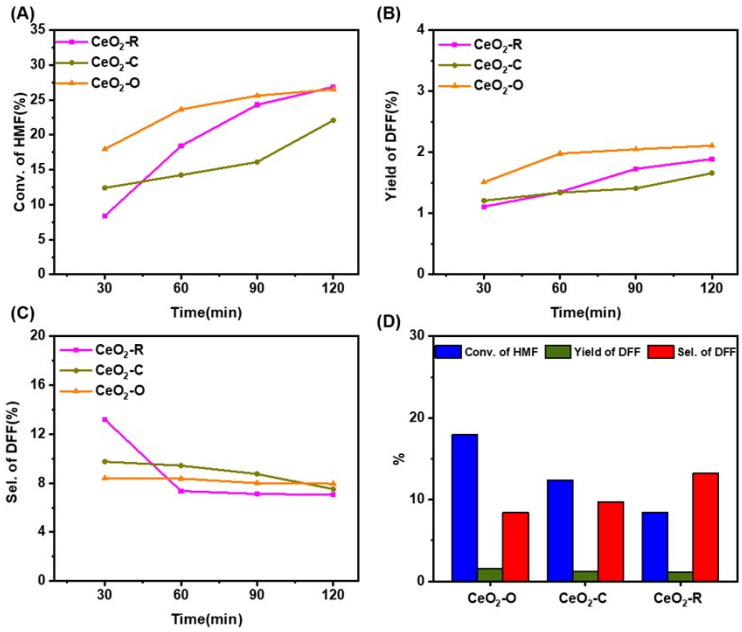

Fig. S36. (A) The conversion rates of HMF. (B) The yield of DFF. (C) The selectivity of DFF. (D) The conversion and selectivity of HMF and DFF for CeO_2-R, CeO_2-C and CeO_2-O.

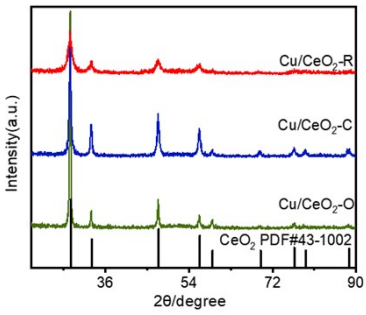

Fig. S37. XRD patterns after photocatalytic HMF oxidation reaction of Cu/CeO_2.

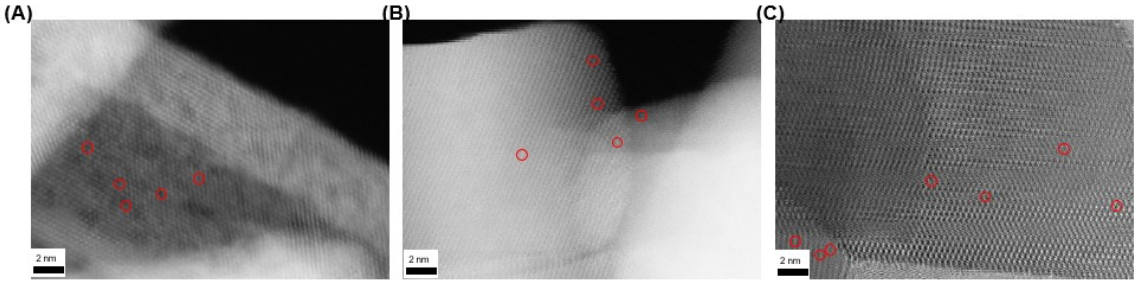

Fig. S38. AC-HAADF-STEM after photocatalytic HMF oxidation reaction of Cu/CeO_2.

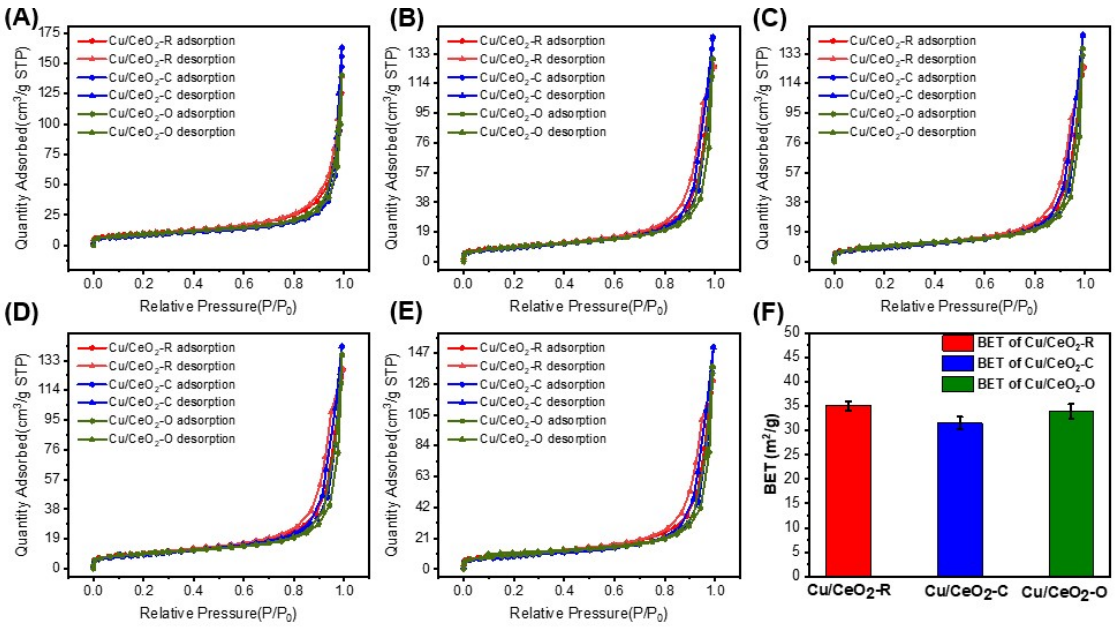

Fig. S39. (A-E) N_2 adsorption-desorption isotherms and (F) histogram of BET surface areas of Cu/CeO_2-R, Cu/CeO_2-C, and Cu/CeO_2-O.

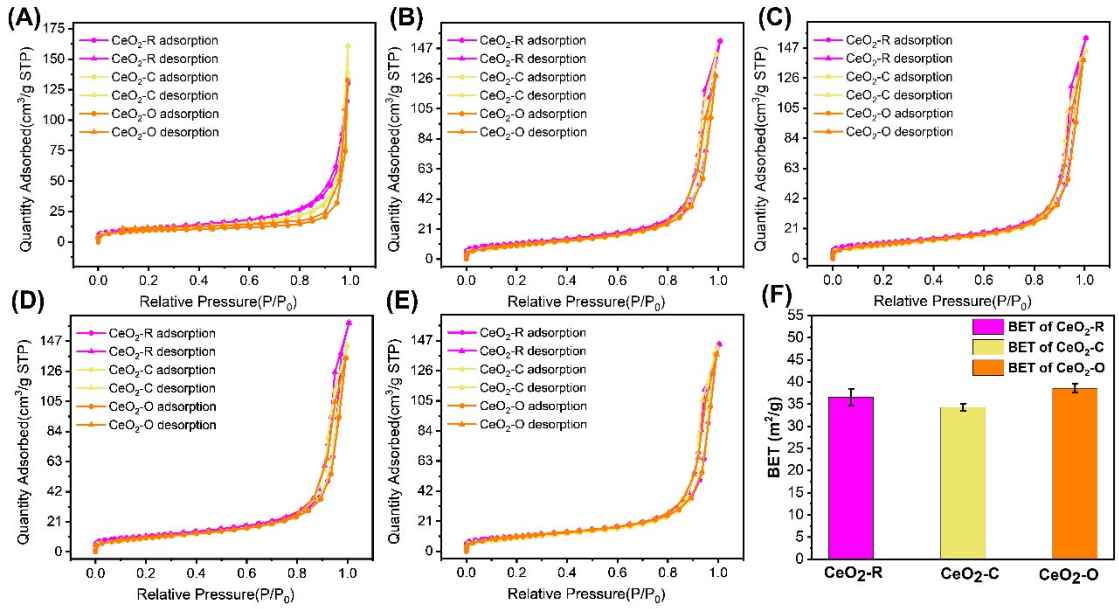

Fig. S40. (A-E) N_2 adsorption-desorption isotherms and (F) histogram of BET surface areas of CeO_2-R, CeO_2-C, and CeO_2-O.

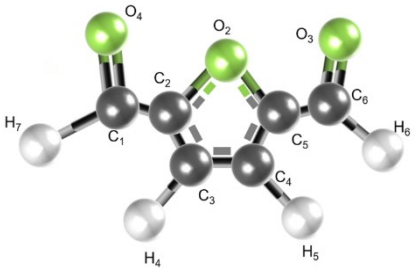

Fig. S41. The structure of DFF.

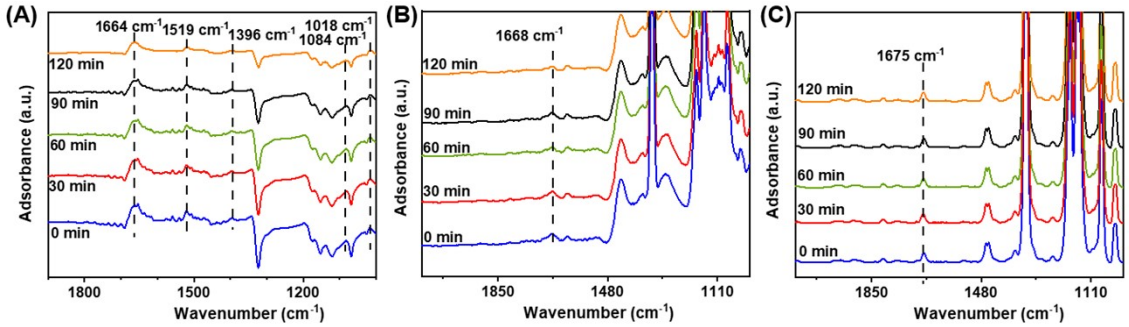

Fig. S42. In-situ DRIFTS of HMF at different time points for (A) CeO_2-R (B) CeO_2-C (C) CeO_2-O (1100-1900 cm^{-1}).

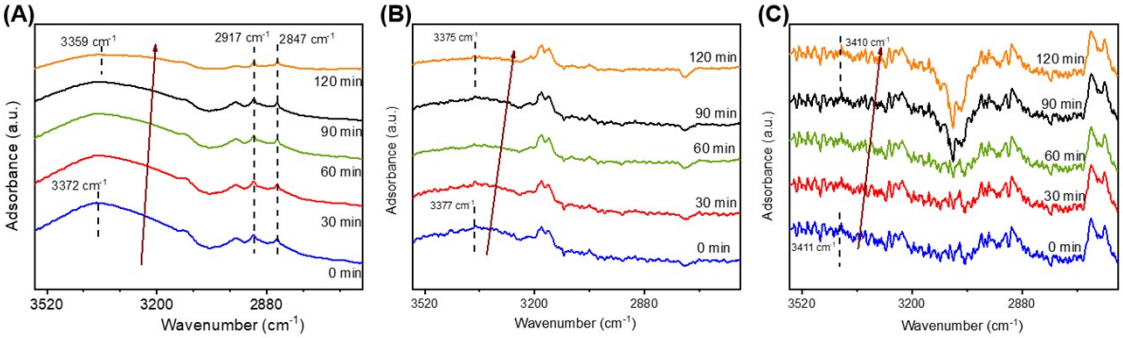

Fig. S43. In-situ DRIFTS of HMF at different time points for (A) CeO_2-R (B) CeO_2-C (C) CeO_2-O (2700-3600 cm^{-1}).

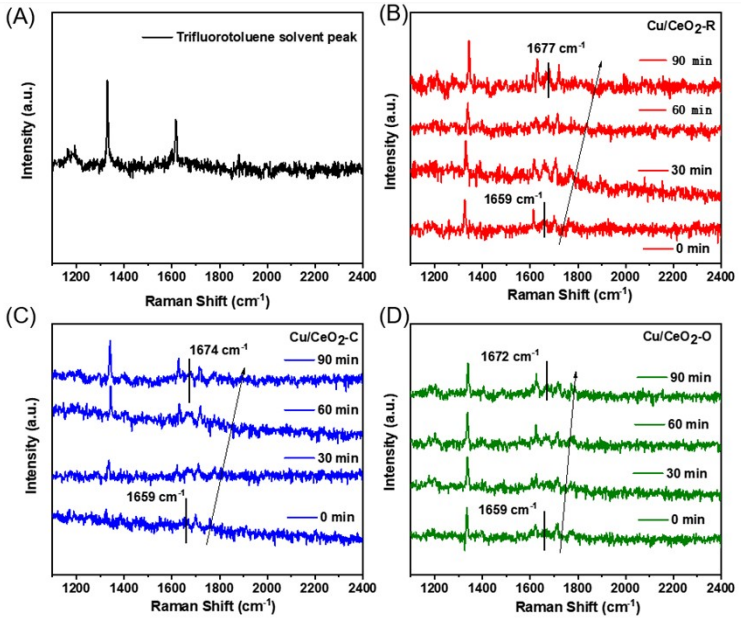

Fig. S44. (A) Trifluorotoluene solvent peak. In-situ Raman of HMF at different time points for (B) Cu/CeO_2-R (C) Cu/CeO_2-C (D) Cu/CeO_2-O.

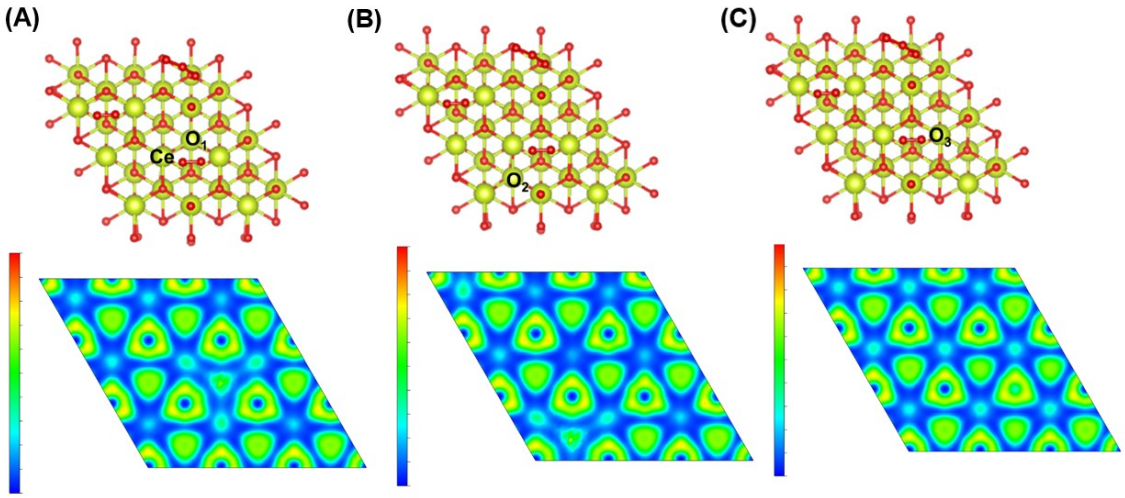

Fig. S45. The electron local density function of the (100) facet removing oxygen at different positions (the closer the color is to red, the more obvious the degree of electron aggregation).

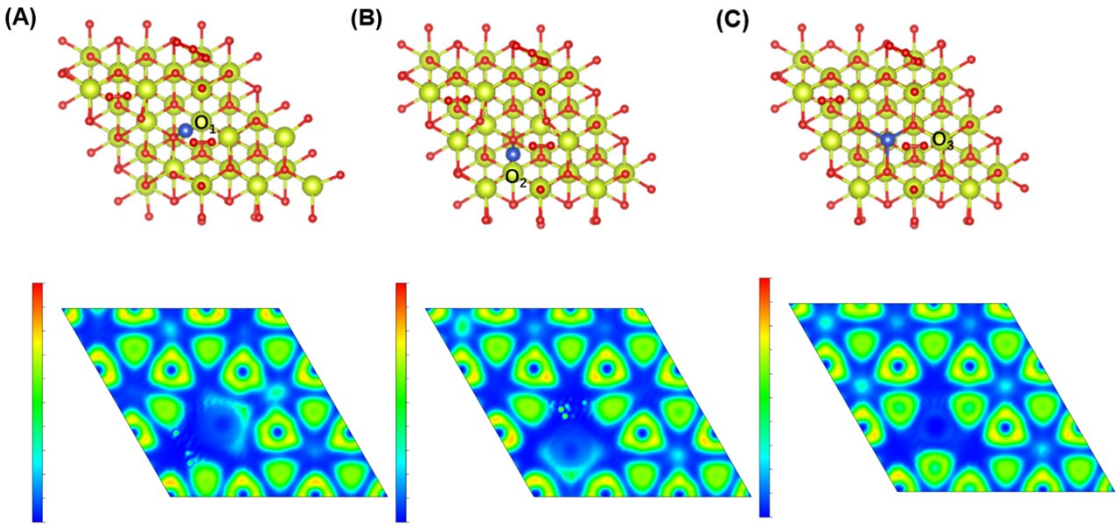

Fig. S46. The electron local density function of the (100) facet removing oxygen and loading Cu at different positions.

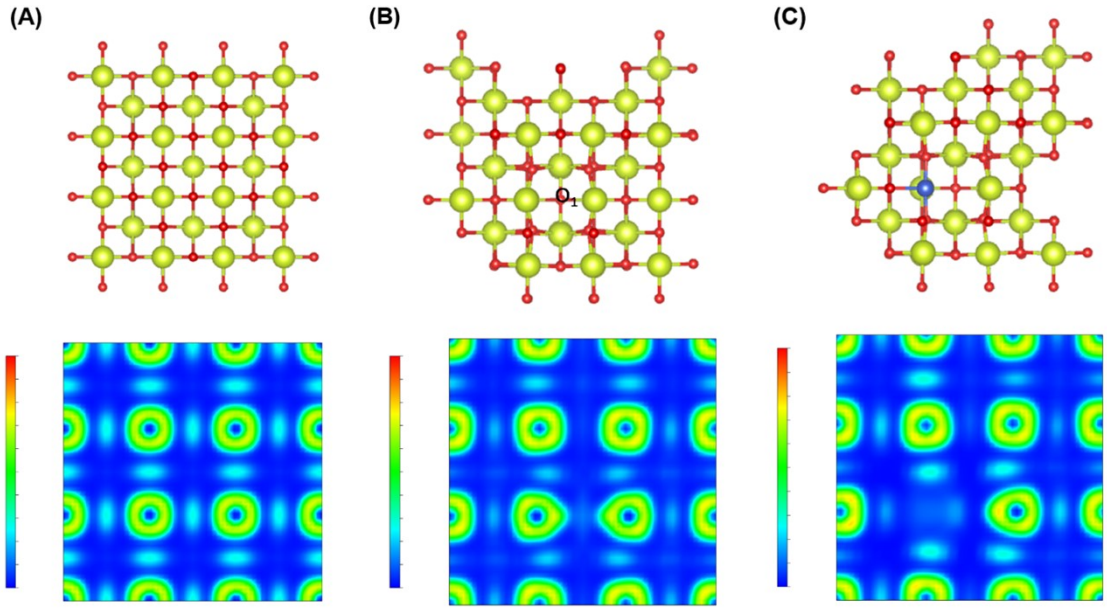

Fig. S47. (A) (110) facet of electron local density function of electrons without removing oxygen from the surface. (B) (110) facet of electron local density function of electrons with removing oxygen from the surface. (C) (110) facet of electron local density function of surface oxygen removed and Cu loaded.

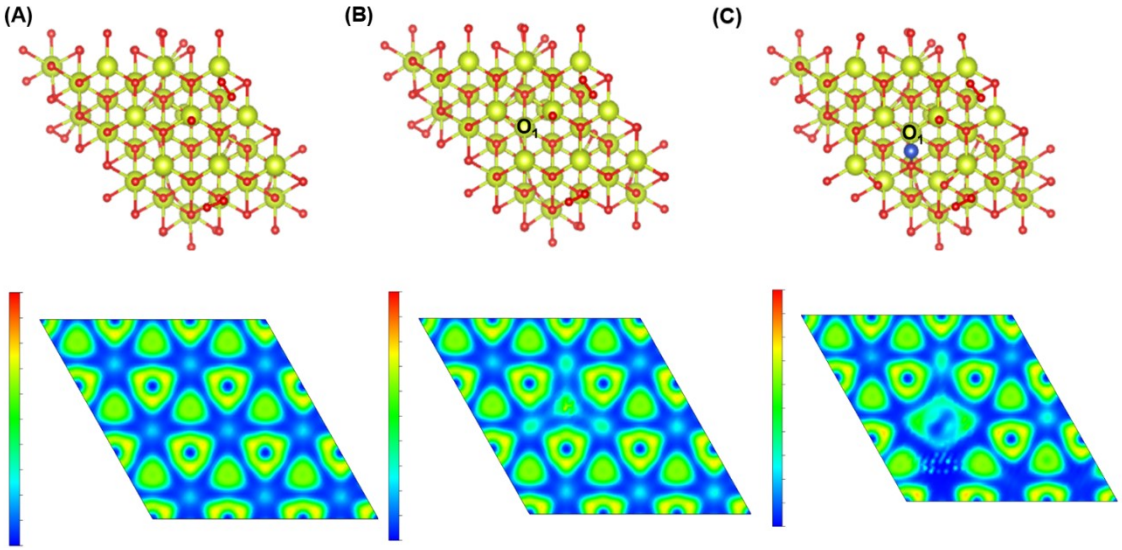

Fig. S48. (A) (111) facet of electron local density function of electrons without removing oxygen from the surface. (B) (111) facet of electron local density function of electrons with removing oxygen from the surface. (C) (111) facet of electron local density function of surface oxygen removed and Cu loaded.

Table S1. EDX and ICP-OES analysis of Cu loading on Cu/CeO_2.

Sample	Cu (EDX) (mol%)	Cu (ICP-OES) (mol%)
Cu/CeO_2-R	4.96	5.03
Cu/CeO_2-C	5.06	5.09
Cu/CeO_2-O	5.02	5.07

Table S2. EDX analysis of CeO_2-O.

Sample	Ce (mol %)	O (mol %)	P (mol %)
CeO_2-O	35.88	64.12	0

Table S3. The peak area of in Ce XPS spectra.

Sample	**Corresponding peak area in Ce^{3+}**	**Corresponding peak area in Ce^{4+}**	**Corresponding peak area in $Ce^{3+}/Ce^{3+}+Ce^{4+}$**
CeO_2-R	156423.49±4421	661410.11±3642	0.2365±0.04
CeO_2-C	138645.47±3212	669875.79±5463	0.1715±0.03
CeO_2-O	52321.46±2605	234621.23±7689	0.1823±0.03
Cu/CeO_2-R	183452.49±4685	688884.59±35461	0.2103±0.04
Cu/CeO_2-C	997865.44±4652	654578.42±46245	0.6038±0.05
Cu/CeO_2-O	172634.38±5647	2524772.25±88654	0.064±0.04

Table S4. The peak area of in O XPS spectra.

Sample	**Corresponding peak area in O_β**	**Corresponding peak area in $O_\beta/O_\alpha+O_\beta+O_\gamma$**
CeO_2-R	108633.26±12933	0.4343±0.12
CeO_2-C	68298.82±5732	0.3682±0.08
CeO_2-O	71101.57±3559	0.3051±0.05
Cu/CeO_2-R	80728.88±4038	0.3776±0.05
Cu/CeO_2-C	46735.2±3271	0.2621±0.07
Cu/CeO_2-O	63023.38±2520	0.2195±0.04

Table S5. The proportion of the Cu XPS spectra.

Sample	**The proportion of Cu^{+}**	**The proportion of Cu^{2+}**
Cu/CeO_2-R	43.35 %±13.10 %	58.68 %±19.65 %
Cu/CeO_2-C	40.37 %±15.35 %	55.83 %±20.48 %
Cu/CeO_2-O	43.29 %±18.53 %	54.61 %±13.27 %

Table S6. Structural parameters of Cu/CeO_2-R, Cu/CeO_2-C and Cu/CeO_2-O references extracted from the quantitative EXAFS curve-fittings.

Sample	Scattering Path	Distance(Å)	C.N.	σ^2(Å^2)	ΔE_0 (eV)	R-factor
Cu/CeO_2-R	Cu-O	1.95	2.9	0.005	-5.69	0.0092
Cu/CeO_2-C	Cu-O	1.96	3.0	0.003	-3.32	0.0021
Cu/CeO_2-O	Cu-O	1.98	3.2	0.004	-3.73	0.0035

Note: C.N.: coordination numbers; Distance: bond distance; σ^2: Debye-Waller factors; ΔE_0: the inner potential correction. R-factor: goodness of fit. EXAFS fitting according to the established Cu/CeO_2-R, Cu/CeO_2-C and Cu/CeO_2-O crystal structures, the S_0^2 was set to 1.

Table S7. EDX results of Pt nanoparticles on Pt/CeO_2.

Sample	Pt loading(wt%)	Dispersion (mol%)
Pt/CeO_2-R	2.61	0.74
Pt/CeO_2-C	1.82	0.52
Pt/CeO_2-O	0.38	0.12

Table S8. EDX results of PbO nanoparticles on PbO/CeO_2.

Sample	Pb loading(wt%)	Dispersion (mol%)
PbO/CeO_2-R	19.80	6.18
PbO/CeO_2-C	5.41	1.78
PbO/CeO_2-O	5.57	1.51

Table S9. Three-finger function fitting parameters of time-resolved fluorescence decay spectra.

Sample	CeO_2-R	CeO_2-C	CeO_2-O	Cu/CeO_2-R	Cu/CeO_2-C	Cu/CeO_2-O
τ_1/ns	0.5846 (97.83%)	0.6058 (97.38%)	0.4715 (95.15%)	0.5769 (91.67%)	0.6157 (97.45%)	0.6219 (100%)
τ_2/ns	3.2980 (2.17%)	3.1375 (2.62%)	2.2006 (4.85%)	2.7742 (8.33%)	3.9023 (2.55%)	0
τ_{ave}/ns	0.6434	0.6721	0.56	0.7599	0.6995	0.6219

Table S10. Conversions of HMF and yields and selectivity of the products for Cu/CeO_2-R.

Time	Conv. of HMF(%)	Yield of DFF(%)	Sel. of DFF(%)	Yield of FFCA(%)	Sel. of FFCA(%)
0.5 h	19.77	18.45	93.34	0.93	4.72
1 h	28.83	25.94	89.97	1.03	3.60
1.5 h	37.35	32.87	88.01	1.33	3.57
2 h	40.2	33.25	82.71	1.42	3.53

Table S11. Conversions of HMF and yields and selectivity of the products for Cu/CeO_2-C.

Time	Conv. of HMF(%)	Yield of DFF(%)	Sel. of DFF(%)	Yield of FFCA(%)	Sel. of FFCA(%)
0.5 h	10.56	3.40	32.22	0.84	7.93
1 h	17.81	5.17	29.03	1.05	5.9
1.5 h	21.44	5.94	27.71	1.08	5.03
2 h	26.28	6.09	23.17	1.29	4.91

Table S12. Conversions of HMF and yields and selectivity of the products for Cu/CeO_2-O.

Time	Conv. of HMF(%)	Yield of DFF(%)	Sel. of DFF(%)	Yield of FFCA(%)	Sel. of FFCA(%)
0.5 h	10.99	1.67	15.20	0.92	8.38
1 h	14.70	1.68	11.37	0.95	6.47
1.5 h	25.61	2.62	10.22	1.02	3.98
2 h	29.62	2.92	9.87	1.17	3.95

Table S13. Conversions of HMF and yields and selectivity of the products for CeO_2-R.

Time	Conv. of HMF(%)	Yield of DFF(%)	Sel. of DFF(%)	Yield of FFCA(%)	Sel. of FFCA(%)
0.5 h	8.40	1.11	13.20	0.48	5.71
1 h	18.41	1.35	7.35	0.97	5.27
1.5 h	24.30	1.73	7.12	1.24	5.11
2 h	26.87	1.89	7.05	1.28	4.76

Table S14. Conversions of HMF and yields and selectivity of the products for CeO_2-C.

Time	Conv. of HMF(%)	Yield of DFF(%)	Sel. of DFF(%)	Yield of FFCA(%)	Sel. of FFCA(%)
0.5 h	12.41	1.21	9.75	1.06	8.50
1 h	14.24	1.34	9.43	1.09	7.65
1.5 h	16.11	1.41	8.75	1.22	7.59
2 h	22.09	1.66	7.51	1.37	6.21

Table S15. Conversions of HMF and yields and selectivity of the products for CeO_2-O.

Time	Conv. of HMF(%)	Yield of DFF(%)	Sel. of DFF(%)	Yield of FFCA(%)	Sel. of FFCA(%)
0.5 h	17.96	1.51	8.41	1.21	6.76
1 h	23.65	1.98	8.37	1.36	5.76
1.5 h	25.61	2.05	8.00	1.46	5.69
2 h	26.53	2.11	7.95	1.51	5.68

Table S16. Comparison of performance of different photocatalysts for photocatalytic oxidation of HMF.

Photocatalyst	**Reaction solution**	**Light source**	**Selectivity of DFF.**	**Ref.**
Pt/ZIS/MnO_2	H_2O	300 W Xe lamp (>400 nm)	85.4%	*Chem. Eng. J.* **2023**, *476*, 146544
P-$Zn_xCd_{1-x}S$	H_2O	LED light (30 × 3 W)	65%	*Appl. Catal., B*. **2018**, *233*, 70−79
CoPz/g-C_3N_4	potassium biphthalate buffer	UV–visible (0.5 W/cm^2)	85%	*J. Am. Chem. Soc.* **2017**, *139*, 14775−14782
TMADT(tetramethylam -monium decatungstate)	acetonitrile (MeCN) + 6 M HBr	Tungsten-bromine lamp (35 W)	76.5%	*Chem. Eng. J.* **2020**, *396*, 125345
g-C_3N_4	H_2O	Philips fluorescent lamp (340-420nm)	35%	*Appl. Catal. B. Environ.* **2017**, *204*, 430−439
Cu/CeO_2-R	benzotrifluoride	300 W Xe lamp (λ ≥ 200 nm)	88.01%	This work

Table S17. BET and standard deviation of Cu/CeO_2.

Sample	BET(m^2/g)	Average value	Standard deviation
Cu/CeO_2-R	35.68	35.10	0.291
	34.37		0.364
	34.31		0.394
	35.08		0.009
	36.05		0.476
Cu/CeO_2-C	30.20	31.55	0.675
	31.80		0.125
	32.05		0.25
	32.32		0.385
	31.38		0.085
Cu/CeO_2-O	32.78	33.30	0.260
	33.42		0.060
	34.79		0.745
	34.13		0.415
	34.63		0.960

Table S18. BET and standard deviation of CeO_2.

Sample	BET(m^2/g)	Average value	Standard deviation
CeO_2-R	39.27	38.59	0.341
	39.01		0.211
	38.95		0.181
	38.97		0.191
	36.74		0.924
CeO_2-C	33.70	34.27	0.286
	34.38		0.054
	34.37		0.049
	35.01		0.369
	33.90		0.186
CeO_2-O	36.04	36.58	0.271
	36.28		0.151
	37.12		0.269
	35.89		0.346
	37.58		0.499

Table S19. The HMF oxidation steps of the catalysts correspond to the energy.

Intermediate products	Cu/CeO_2-R	Cu/CeO_2-C	Cu/CeO_2-O	CeO_2-R	CeO_2-C	CeO_2-O
*HMF	-1.75	-0.76	-0.88	-1.74	-0.85	-0.49
*HMF-H^+	-1.27	-1.37	-3.31	-2.73	1.81	-2.61
*DFF	-0.34	-0.35	-1.83	-0.89	-2.43	-1.55

Reference

1 H. X. Mai, L. D. Sun, Y. W. Zhang, R. Si, W. Feng, H. P. Zhang, H. C. Liu, C. H. Yan, Shape-selective synthesis and oxygen storage behavior of ceria nanopolyhedra, nanorods, and nanocubes. *J. Phys. Chem. B* 2005, **109**, 24380−243855.

2 L. Yan, R. Yu, J. Chen, X. Xing, Template-free hydrothermal synthesis of CeO_2 nano-octahedrons and nanorods: investigation of the morphology evolution. *Cryst. Growth Des*. 2008, **8**, 1474−1477.

3 L. Liu, M. Y. Gao, H. Yang, X. Wang, X. Li, Linear Conjugated Polymers for Solar-Driven Hydrogen Peroxide Production: The Importance of Catalyst Stability. *J. Am. Chem. Soc*. 2021, **143**, 19287-19293.

4 Z. F. Yang, X. N. Xia, M. Fang, L. L. Wang, Y. T. Liu, Photothermal effect act as controllable switch for tunable photocatalytic selective oxidation of 5-Hydroxymethylfurfural. *Chem. Eng. J*. 2023, **476**, 146544.

5 H. F. Ye, R. Shi, X. Yang, W. F. Fu, Y. Chen, P-doped $Zn_xCd_{1-x}S$ solid solutions as photocatalysts for hydrogen evolution from water splitting coupled with photocatalytic oxidation of 5-hydroxymethylfurfural. *Appl. Catal., B*. 2018, **233**, 70−79.

6 S. Xu, P. Zhou, Z. Zhang, C. Yang, B. Zhang, K. Deng, S. Bottle, H. Zhu, Selective Oxidation of 5-Hydroxymethylfurfural to 2,5-Furandicarboxylic Acid Using O_2 and a Photocatalyst of Co-thioporphyrazine Bonded to g-C_3N_4. *J. Am. Chem. Soc.* 2017, **139**, 14775−14782.

7 B. H. Yang, W. W. Wan, F. F. Zhang, C. Fu, Z. H. Su, A. Q. Adjusting effect of additives on decatungstate-photocatalyzed HMF oxidation with molecular oxygen under visible light illumination. *Chen, Chem. Eng. J.* 2020, 396, 125345.

8 I. Krivtsov, E. Garcia-Lopez, G. Marci, L. Palmisano, Z. Amghouz, J. Garcia, S. Ordonez, E. Diaz, Selective photocatalytic oxidation of 5-hydroxymethyl-2-furfural to 2,5-furandicarboxyaldehyde in aqueous suspension of g-C_3N_4. *Appl. Catal. B. Environ*. 2017, **204**, 430−439.